



HAL
open science

Venus OH nightglow distribution based on VIRTIS limb observations from Venus Express

Lauriane Soret, Jean-Claude Gérard, Giuseppe Piccioni, Pierre Drossart

► To cite this version:

Lauriane Soret, Jean-Claude Gérard, Giuseppe Piccioni, Pierre Drossart. Venus OH nightglow distribution based on VIRTIS limb observations from Venus Express. *Geophysical Research Letters*, 2010, 37, pp.06805. 10.1029/2010GL042377 . hal-03743141

HAL Id: hal-03743141

<https://hal.science/hal-03743141>

Submitted on 19 Aug 2022

HAL is a multi-disciplinary open access archive for the deposit and dissemination of scientific research documents, whether they are published or not. The documents may come from teaching and research institutions in France or abroad, or from public or private research centers.

L'archive ouverte pluridisciplinaire **HAL**, est destinée au dépôt et à la diffusion de documents scientifiques de niveau recherche, publiés ou non, émanant des établissements d'enseignement et de recherche français ou étrangers, des laboratoires publics ou privés.

Copyright



Venus OH nightglow distribution based on VIRTIS limb observations from Venus Express

L. Soret,¹ J.-C. Gérard,¹ G. Piccioni,² and P. Drossart³

Received 6 January 2010; revised 10 February 2010; accepted 16 February 2010; published 24 March 2010.

[1] The full set of VIRTIS-M limb observations of the OH Venus nightglow has been analyzed to determine its characteristics. Based on 3328 limb profiles, we find that the mean peak intensity along the line of sight of the OH($\Delta v = 1$ sequence) is $0.35_{-0.21}^{+0.53}$ MR and is located at 96.4 ± 5 km. The emission is highly variable and no dependence of the airglow layer altitude versus the antisolar angle is observed. The peak brightness appears to decrease away from the antisolar point even if the variability at a given location is very strong. Some correlation between the intensity of the OH and the O₂(a¹Δ) emissions is also observed, presumably because atomic oxygen is a common precursor to the formation of O₂(a¹Δ) and O₃, whose reaction with H produces excited OH. Comparing our results with predictions from a photochemical model, a constant H flux does not match the simultaneous OH and O₂ airglow observations.

Citation: Soret, L., J.-C. Gérard, G. Piccioni, and P. Drossart (2010), Venus OH nightglow distribution based on VIRTIS limb observations from Venus Express, *Geophys. Res. Lett.*, *37*, L06805, doi:10.1029/2010GL042377.

1. Introduction

[2] The first identification of the OH airglow in the terrestrial mesosphere was made in 1950 by Meinel [1950]. It is generated by the reaction between ozone and hydrogen atoms leading to the production of vibrationally excited hydroxyl molecules in the X²Π state. Recently, the unexpected presence of the OH nightglow was observed in the Venus mesosphere by Piccioni *et al.* [2008] using a limb profile from the Visible and Infra-Red Thermal Imaging Spectrometer (VIRTIS) instrument on board the Venus Express spacecraft. They clearly identified the (1-0) and (2-1) transitions at 2.80 and 2.94 μm, respectively and the (2-0) band at 1.43 μm. Additional bands belonging to the Δv = 1 sequence also appear to be present longward of the (1-0) band. The maximum intensity in the limb viewing geometry was 0.88 ± 0.09 MR (1 Rayleigh, R, corresponds to the brightness of an extended source emitting 10⁶ photons cm⁻² s⁻¹ in 4π sr) and located at 96 ± 2 km. In a preliminary study of characteristics of the OH emission distribution, Gérard *et al.* [2010] found an average brightness of about 0.41 ± 0.37 MR peaking at 95.3 ± 3 km. They also pointed out a correlation between the OH(Δv = 1 sequence) and

the O₂(a¹Δ) nightglow intensities. Krasnopolsky [2010] recently obtained infrared spectra from ground based observations of the (1-0) P1(4.5) and (2-1) Q1(1.5) OH airglow lines using a high-resolution telescope and long exposure times. He used these measurements to constrain a one-dimensional photochemical model for the nighttime atmosphere of Venus. He derived expressions linking the brightness of the OH and the O₂(a¹Δ) emissions to the downward flux of oxygen and hydrogen atoms. On the Venus nightside, the OH emission is weak compared to the thermal emission of the planet. This weakness combined with both the lower spectral resolution of VIRTIS-M and its short exposure times make it impossible to detect an OH emission in nadir geometry. Only limb observations can thus be used in this study. Here, we determine the global distribution of the Venus OH nightglow using VIRTIS observations following appropriate corrections to the limb observations. We use the full data set collected during the Venus Express mission.

2. Limb Observations of the OH(Δv = 1) Night Airglow

[3] Venus Express is a spacecraft of the European Space Agency orbiting Venus on an elliptical trajectory with a pericenter situated at high northern latitudes and an apocenter located 66,000 km away from the planet. VIRTIS-M-IR is an imaging spectrometer covering the infrared domain from 1 to 5 μm both in nadir and limb viewing geometries [Drossart *et al.*, 2007; Piccioni *et al.*, 2009]. Because of the spacecraft's polar elliptical orbit, limb measurements are preferentially made while VIRTIS is observing the northern hemisphere. For this study we used VIRTIS-M-IR observations from 14 April 2006 (orbit VI0023_01) to 14 October 2008 (orbit VI0907_05). During this period, a total of 4501 observations were collected. Since VIRTIS-M-IR is an imaging spectrometer, a single observation consists of an image cube for each spectral channel, from 1 to 5 μm, by steps of 9.5 nm. It is thus possible to obtain complete spectra, where the O₂(a¹Δ - X³Σ) and the OH(Δv = 1) Meinel bands can clearly be seen at 1.27 and from 2.7 to 3.1 μm, respectively [Piccioni *et al.*, 2008]. Limb emission profiles of the OH(Δv = 1) emission can also be deduced from these observations.

[4] Gérard *et al.* [2010] described the procedure applied to extract limb profiles from VIRTIS images. First, images are integrated pixel per pixel over wavelengths from 2.7 to 3.1 μm. Then, all the intensities of pixels with identical latitudes and local times but different altitudes are grouped together to ultimately obtain an intensity profile as a function of the altitude of the minimum ray height. Occasionally, the OH peak intensity is too weak to be distinguished from the

¹Laboratoire de Physique Atmosphérique et Planétaire, Université de Liège, Liège, Belgium.

²IASF, INAF, Rome, Italy.

³Observatoire de Paris, Meudon, France.

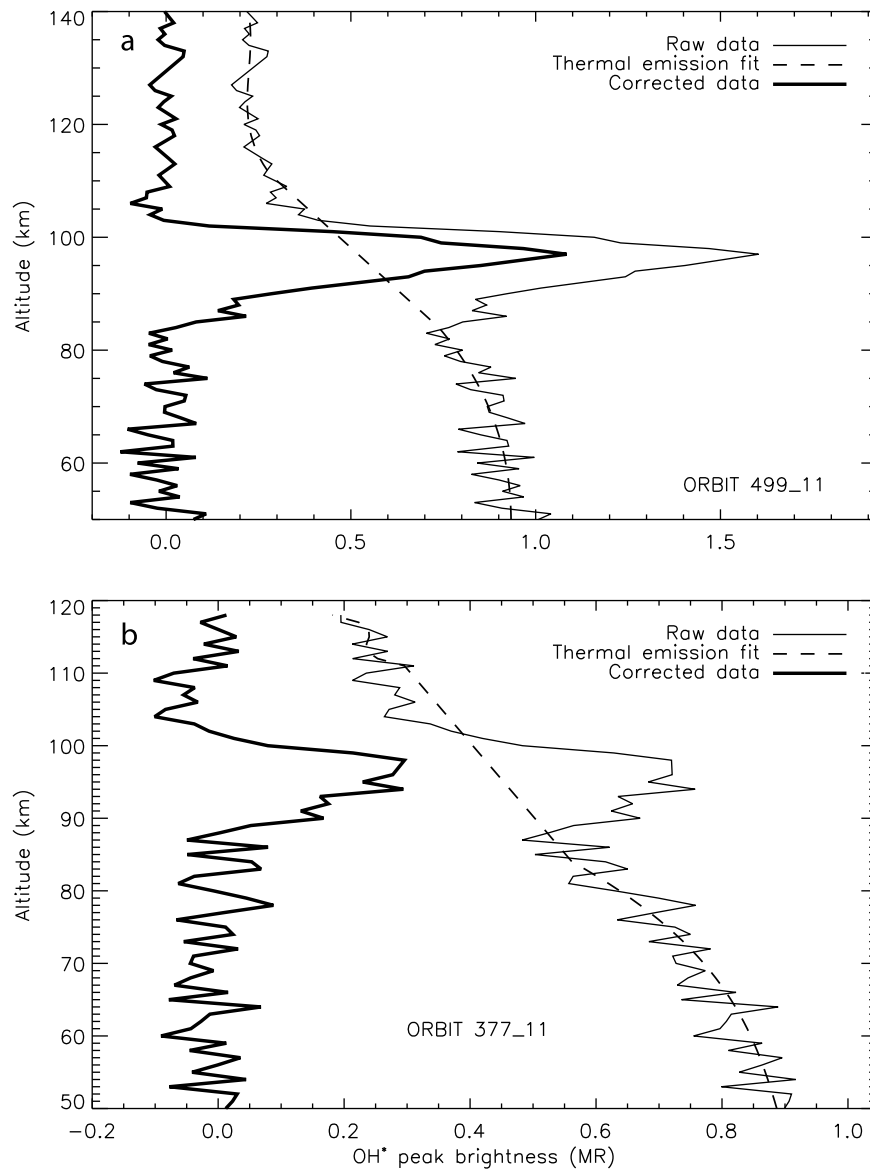


Figure 1. Limb profiles derived from orbits VI0499_11 (a) and 377_11 (b): raw data (thin solid line), Venus’s thermal emission (fit in dashed line) and OH($\Delta v = 1$) emission (thick solid line).

thermal contribution. For that analysis, a selection has been made to only keep those profiles exhibiting a discernable emission peak. An example of a bright OH limb profile is plotted in Figure 1a (thin solid line) while a weaker case is represented in Figure 1b. As can be seen, in addition to the OH emission, a contribution presumably caused by scattering of thermal emission by haze has to be removed from the original profile. To do so, a third-order polynomial fit was applied to represent the thermal emission above 110 km. The same procedure was applied to fit the thermal emission below 85 km. The two polynomial fits are subsequently smoothly connected. The final curve used to fit the thermal emission is plotted in dashed line and the thick solid line shows the corrected OH emission profile. To verify that both polynomials fit the thermal component of the profiles, boundaries of 85 and 110 km have been chosen because no emission peak has been found out of this range (see

Figure 2a). Although this method works really well for bright profiles (see Figure 1a), the accuracy of the results had to be tested for weaker emissions. In the case of Figure 1b, it clearly appears that using boundaries of 85 and 104 km would have provided a better fit of the thermal emission. The peak emission is then found to be 0.34 MR instead of 0.30 MR for the automatic method, which leads to a relative peak intensity error of 11%. Because this uncertainty is sufficiently low and considering the large amount of profiles to be analyzed, we use the automatic procedure for all profiles. From now on, only the OH corrected profiles and the data concerning the altitude and the brightness of the peak will be taken into account. In this study, we verify that all available limb profiles are considered and corrected for the thermal emission component. While an earlier study by *Gérard et al.* [2010] was based on 334 OH limb profiles, this work is based on a total of 3618 visually checked

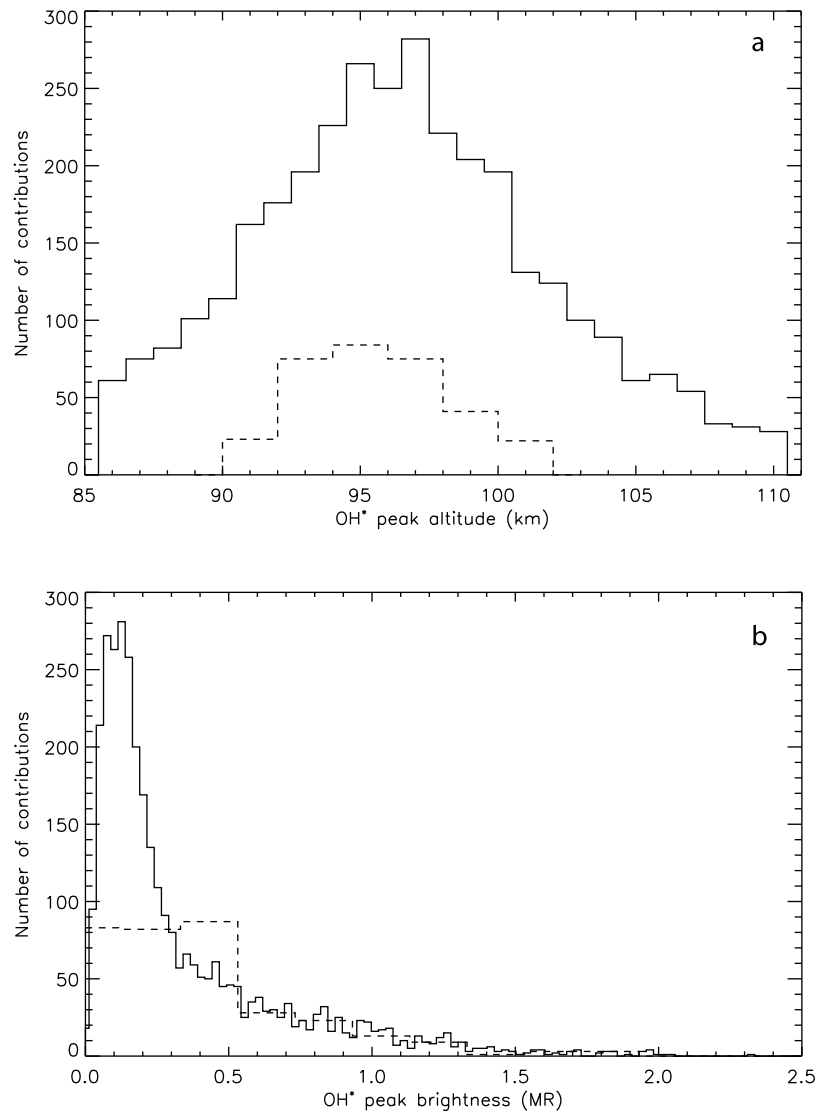


Figure 2. Distribution of the peak (a) altitude and (b) brightness along the line of sight of the nightside OH($\Delta v = 1$) emission observed at the limb with VIRTIS-M-IR. As a comparison, results previously obtained by *Gérard et al.* [2010] are represented with dashed lines.

profiles. Among these, 290 profiles have been rejected either because they were too noisy or because the fit to the thermal emission was not satisfactory.

3. Results

3.1. OH($\Delta v = 1$) Nightglow Distribution

[5] The statistics of the values of the peak altitude and of the peak brightness is shown in Figure 2 with solid lines while previous results obtained by *Gérard et al.* [2010] are represented in dashed lines. In Figure 2a, the mean of the OH peak altitude along the line of sight is found to be 96.4 ± 5 km (versus 95.3 ± 3 km for the study by *Gérard et al.* [2010]), with a minimum value of 86 km, a maximum value of 110 km (versus 102 km), a median of 96 km and a mode (the most represented value) of 97 km. Comparison of the two histograms shows that increasing the number of profiles does not appreciably change the peak altitude distribution. In Figure 2b, the mean of the OH maximum

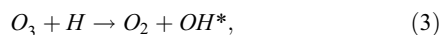
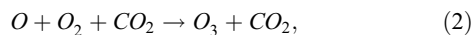
brightness along the line of sight is found to be 0.35 MR (versus 0.41 ± 0.37 MR in *Gérard et al.* [2010]), ranging from values below detection up to 2.3 MR (versus tens of kiloRayleighs to 2 MR), with a median value of 0.21 MR and a mode of 0.14 MR (versus 0.4 MR). As the brightness distribution is asymmetric, the variability is $0.35^{+0.53}_{-0.21}$ MR, asymmetrically expressed as well. This mean value drops to $0.32^{+0.53}_{-0.21}$ MR when considering all the rejected profiles as zero values. Comparing both histograms shows that removing thermal emission from limb profiles adds smaller intensity values but does not appreciably modify the shape of the largest intensity distribution.

[6] Another interesting aspect is the spatial representation of the peak altitude and intensity values. We considered the brightness of the OH emission as a function of latitude sorted into 5° -wide bins. From 20°S to 80°N , a tendency to decrease (from 0.55 to 0.15 MR) is obtained (not shown), with a correlation coefficient R equal to -0.55 . To test the significance of this correlation, a correlation coefficient $r =$

−0.07 was also calculated using all the individual data points (unbinned). To assess the significance of this correlation coefficient, the null hypothesis has to be tested. Since the number of samples exceeds 100, r is normally distributed around 0 for two non-correlated variables and the standard deviation of r is given by $s_0 = 1/\sqrt{n-1}$, where n is the number of observations. Comparing the r value to s_0 , the level of confidence that r is significantly different from zero is found to exceed 99.99%. Similarly, the brightness of the OH emission has been examined as a function of local time using 15 min local time bins (not shown). In this case, an intensity increase from 0.30 to 0.40 MR from dusk to dawn was obtained, leading to $R = 0.40$, $r = -0.13$ and a level of confidence that r is significantly different from zero exceeding 99.99%. However, the observations used for these analyses are not uniformly distributed either in latitude or local time. Thus, the bins do not contain the same number of observations, varying from 4 to 405 profiles per bin. Selecting observations along concentric circles around the antisolar point (whose coordinates are 0° lat – 2400 local time) has been used to avoid this issue. This variable, known as the angular distance to the antisolar point (or antisolar angle), was shown to be very useful to organize the $O_2(a^1\Delta)$ airglow brightness data [Gérard *et al.*, 2010]. Figure 3a shows that the number of observations per bin is less variable, varying from 21 to 333 profiles per bin. Figure 3b clearly shows that the intensity is significantly brighter near the antisolar point (about 0.6 MR) than near the poles (about 0.3 MR). The corresponding correlation coefficients are found to be $R = -0.71$ and $r = -0.02$. In this case, the level of confidence that r is significantly different from zero is about 77%. For its part, the altitude of the peak emission appears to exhibit no dependence on latitude, local time or antisolar angle (Figure 3c).

3.2. OH Meinel and $O_2(a^1\Delta)$ Simultaneous Observations

[7] Another important aspect is the possible correlation between the OH($\Delta v = 1$) and the $O_2(a^1\Delta)$ emissions. Indeed, they are linked by the following reactions:



where O_2^* and OH^* designate the $O_2(a^1\Delta)$ and OH($v = 1$) excited states, respectively. Thus, excited OH is produced with the quick consumption of ozone, created itself by the termolecular reaction involving O, O_2 and a third body. Considering these mechanisms, a correlation between the OH($\Delta v = 1$) and the $O_2(a^1\Delta)$ emissions is expected.

[9] To compare the two emissions, O_2 profiles have been extracted following the same procedure as the OH profiles, but no thermal emission correction was needed. Indeed, the $O_2(a^1\Delta)$ signal at $1.27 \mu\text{m}$ is considerably stronger than the OH emission. Also, the thermal emission in this channel is comparatively very weak above 85 km [Piccioni *et al.*,

2009] while the O_2 emission peak is observed near 96 km [Piccioni *et al.*, 2009; Gérard *et al.*, 2008]. Each data point in Figure 4 represents the peak brightness measured along the line of sight of the OH($\Delta v = 1$) and the $O_2(a^1\Delta)$ emissions for simultaneous limb observations. The plot (solid line) and the linear correlation coefficient $r = 0.47$ (with a confidence level that the correlation coefficient is different from zero exceeding 99.99%) both suggest that the brightness of the OH and the $O_2(a^1\Delta)$ emissions tends to statistically covary.

[10] Krasnopolsky [2010] presented a one-dimensional photochemical-transport model of the photochemistry between 80 and 130 km. He suggested that the OH brightness is linked to the $O_2(a^1\Delta)$ brightness and the downward flux of hydrogen atoms through:

$$I_{OH} = 1.3 \left\{ 1.2 \left[\frac{\Phi_O}{10^{12}} \right]^{1.46} \left[\frac{\Phi_H}{10^8} \right]^{0.46 - 0.048 \ln \left(\frac{\Phi_H}{10^8} \right)} \right\}, \quad (5)$$

$$\Phi_O = \left(\frac{I_{O_2}}{0.158} \right)^{1/1.14} \times 10^{12}, \quad (6)$$

where I_{OH} is the nadir brightness of the OH($\Delta v = 1$) emission in kR, I_{O_2} is the nadir brightness of the $O_2(a^1\Delta)$ emission in MR, Φ_O and Φ_H are the oxygen and the hydrogen vertical fluxes at 130 km expressed in $\text{cm}^{-2} \text{s}^{-1}$, respectively. The nadir observations of the OH and the O_2 intensities made by Krasnopolsky [2010] at 2130 LT between 35°N and 35°S have been converted into limb intensities and represented in Figure 4 by a square. He deduced from a comparison with the model outputs that a hydrogen flux in equation (5) equal to $10^8 \text{ cm}^{-2} \text{ s}^{-1}$ best fits this observation. The model relation between the $O_2(a^1\Delta)$ and the OH Meinel brightness derived from (5) and (6) for this H flux value is represented in dashed line in Figure 4. This curve passes through Krasnopolsky's observation but does not fit well the high O_2 brightness values which were not considered in his study. Curves for other values of the hydrogen flux have been plotted for comparison. It appears that a hydrogen flux of $10^8 \text{ cm}^{-2} \text{ s}^{-1}$ seems appropriate to fit the lowest values of the $O_2(a^1\Delta)$ emission while a smaller value of $3 \times 10^7 \text{ cm}^{-2} \text{ s}^{-1}$ (in dashed-dotted line) seems to better fit the highest intensities. However, some points, with low O_2 values but OH intensities greater than 1.5 MR, are not fitted, whatever the hydrogen flux. A detailed inspection of the corresponding spectra confirmed the relatively high OH to O_2 intensity ratio. These points only represent less than 0.7% of all the observations.

4. Conclusions

[11] The entire data set of VIRTIS-M-IR limb observations of the OH nightglow obtained during the Venus Express mission has been analyzed for this study. To correctly estimate the brightness of the OH($\Delta v = 1$) Meinel emission, the contribution of the thermal emission has been subtracted. This process resulted in increasing the number of profiles compared to earlier preliminary studies and adding lower OH intensity values to the data set. Our study indicates that, globally, the observed peak brightness of the OH Meinel

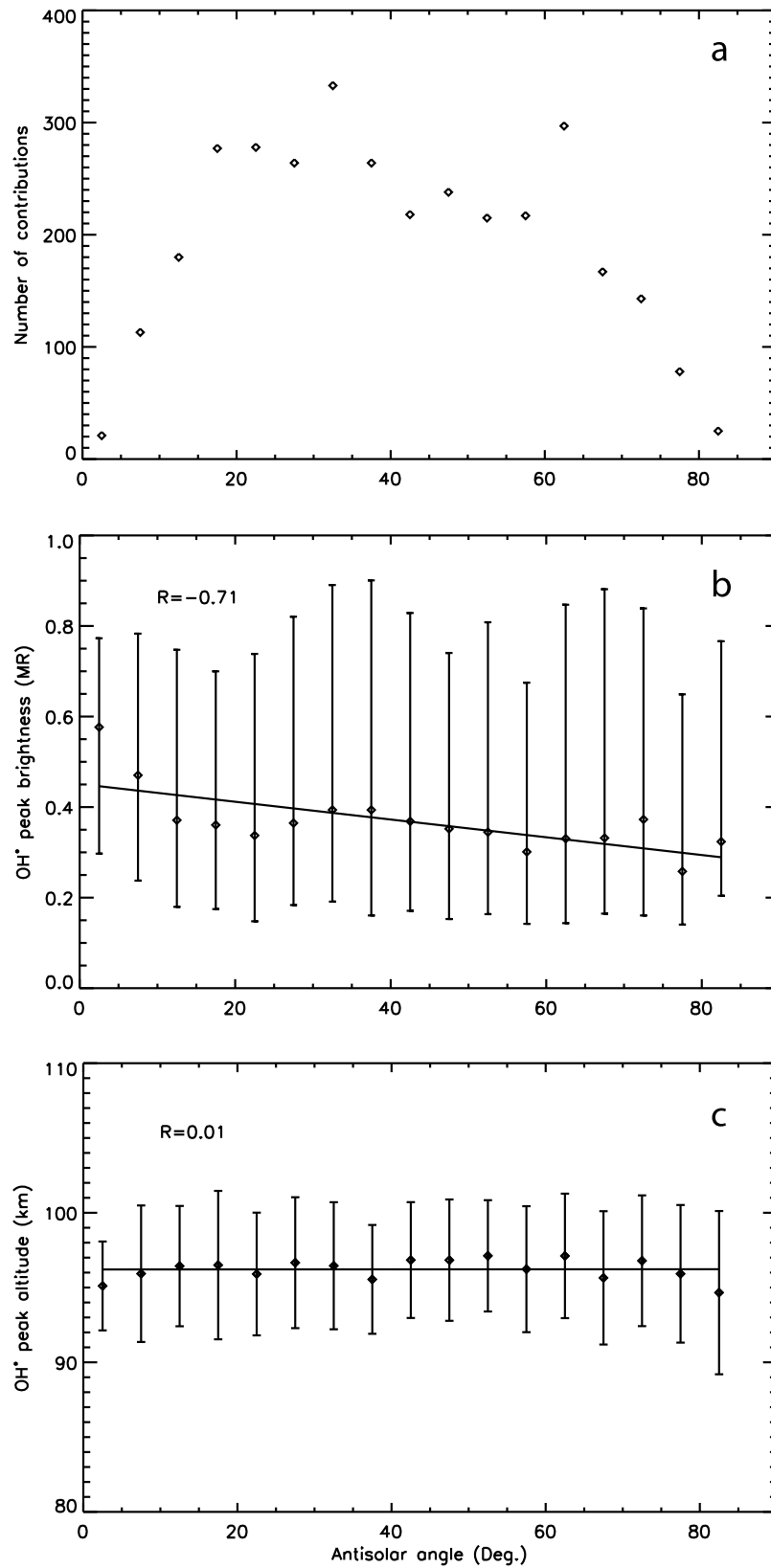


Figure 3. (a) Statistical distribution of the number of OH($\Delta v = 1$) infrared nightglow observations grouped into 5° angular bins. The maximum limb (b) brightness and (c) altitude are plotted as a function of the antisolar angle. The central values in each bin are the mean values and the vertical bars indicate the asymmetric variability in each bin. The solid line shows the linear regression through the binned data points and the value of the linear correlation coefficient R for the binned data is indicated.

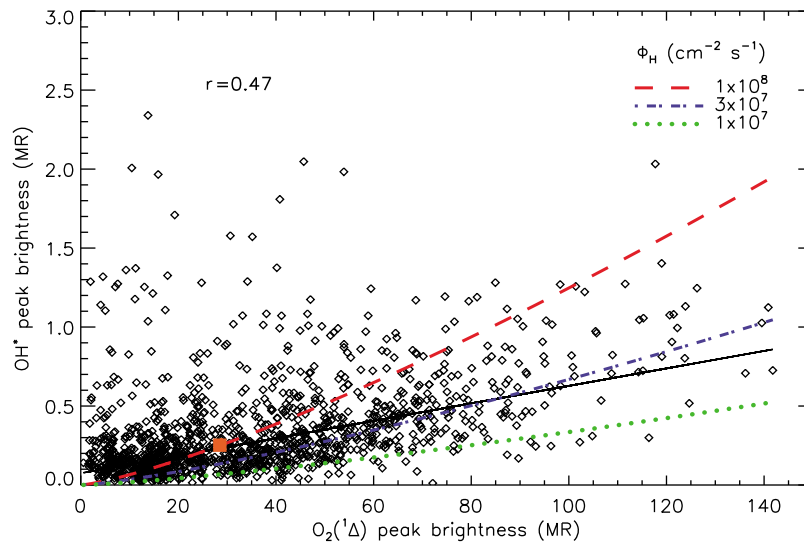


Figure 4. Relationship between the maximum limb brightness of individual simultaneous OH and $O_2(a^1\Delta)$ limb profiles. The regression line through the data points is plotted in a black solid line and the value of the correlation coefficient r is indicated. The square represents the observation of *Krasnopolsky* [2010] at 2130 LT. The dashed line represents the calculated relationship for a downward hydrogen flux of 10^8 atoms $\text{cm}^{-2} \text{s}^{-1}$ at 130 km.

emission at the limb is very variable, ranging from less than 20 kR to about 2 MR.

[12] Statistics indicate that the OH intensity tends to be brighter near the antisolar point than near the poles, although the associated level of confidence is low when individual measurements are considered. This relatively low level of the correlation stems from the extreme variability in individual observations, which is neither apparent in the binned data nor in the preliminary results by *Gérard et al.* [2010] based on a limited sample. Our results indicate that, as more OH observations are considered, the associated variability increases. By contrast, although the OH peak altitude also appears to be variable, it shows no dependence with the location on the nightside of Venus.

[13] Some degree of correlation is expected between the brightness of the OH and the O_2 emissions which have atomic oxygen as a common reactant in reactions (1) and (4) and as a precursor to ozone involved in reaction (3). This relationship was numerically predicted by the nightside model by *Krasnopolsky* [2010] for a given value of the downward fluxes of O and H atoms. Our results suggest that the hydrogen flux is not constant. A hydrogen flux of $10^8 \text{ cm}^{-2} \text{ s}^{-1}$ best fits $O_2(a^1\Delta)$ intensities from 0 to 40 MR, while a smaller value of $3 \times 10^7 \text{ cm}^{-2} \text{ s}^{-1}$ better reproduces the higher brightness data (see Figure 4). As the highest $O_2(a^1\Delta)$ intensity values are statistically located near the antisolar point and decrease toward the poles [*Piccioni et al.*, 2009; *Gérard et al.*, 2008], this could imply that the hydrogen flux is larger near the pole than near the antisolar point. However, we note that, globally, the intensity level of the OH nightglow is correctly predicted by the one-dimensional model of Venus's nightside photochemistry. Finally, it is important to keep in mind that horizontal transport plays an important role in the redistribution of photochemically-produced species such as O, O_3 and minor long-lived species and possibly explains some of the vari-

ability of the OH emission and its brightness relative to $O_2(a^1\Delta)$.

[14] **Acknowledgments.** We gratefully thank all members of the ESA Venus Express project and of the VIRTIS scientific and technical teams. L. Soret was supported by the PRODEX program managed by the European Space Agency with the help of the Belgian Federal Space Science Policy Office. J.-C.G. acknowledges funding from the Belgian Fund for Scientific Research (FNRS). This work was funded by Agenzia Spaziale Italiana and the Centre National d'Etudes Spatiales.

References

- Drossart, P., et al. (2007), Scientific goals for the observation of Venus by VIRTIS on ESA/Venus Express mission, *Planet. Space Sci.*, 55, 1653–1672, doi:10.1016/j.pss.2007.01.003.
- Gérard, J.-C., A. Saglam, G. Piccioni, P. Drossart, C. Cox, S. Erard, R. Hueso, and A. Sánchez-Lavega (2008), Distribution of the O_2 infrared nightglow observed with VIRTIS on board Venus Express, *Geophys. Res. Lett.*, 35, L02207, doi:10.1029/2007GL032021.
- Gérard, J.-C., L. Soret, A. Saglam, G. Piccioni, and P. Drossart (2010), The distributions of the OH Meinel and $O_2(a^1\Delta-X^3\Sigma)$ nightglow emissions in the Venus mesosphere based on VIRTIS observations, *Adv. Space Res.*, doi:10.1016/j.asr.2010.01.022, in press.
- Krasnopolsky, V. A. (2010), Venus night airglow: ground-based detection of OH, Observations of O_2 emissions, and photochemical model, *Icarus*, doi:10.1016/j.icarus.2009.10.019.
- Meinel, A. B. (1950), OH emission bands in the spectrum of the night sky, *Astrophys. J.*, 111, 555, doi:10.1086/145296.
- Piccioni, G., et al. (2008), First detection of hydroxyl in the atmosphere of Venus, *Astron. Astrophys.*, 483, L29–L33, doi:10.1051/0004-6361:200809761.
- Piccioni, G., L. Zasova, A. Migliorini, P. Drossart, A. Shakun, A. García Muñoz, F. P. Mills, and A. Cardesín-Moinelo (2009), Near-IR oxygen nightglow observed by VIRTIS in the Venus upper atmosphere, *J. Geophys. Res.*, 114, E00B38, doi:10.1029/2008JE003133.
- P. Drossart, Observatoire de Paris, 5 place Jules Janssen, F-92195 Meudon CEDEX, France.
- J.-C. Gérard and L. Soret, Laboratoire de Physique Atmosphérique et Planétaire, Université de Liège, 17, Allée du 6 Aout, B-4000 Liège, Belgium. (lauriane.soret@ulg.ac.be)
- G. Piccioni, IASF, INAF, Via del Fosso del Cavaliere 100, I-00133 Roma, Italy.